AADE-12-FTCE-20

Investigating Fluid Invasion into Formations Using Exponential Shear

Jason Maxey and Ryan van Zanten, Halliburton

Abstract

Fluid invasion into formations while drilling is a common issue and is often sought to be minimized in order to reduce the possibility of weakening the borehole or potentially plugging the production zone. In other cases, fluid invasion is desired as we seek to place lost circulation material, perform wellbore strengthening, or control flow through a frac pack. Often assumed to be a simple shear flow as through a bundle of various sized tubes, flow in porous media is in reality tortuous, through converging and diverging channels which induce mixed shear and extensional flows on the fluid. The behavior of fluids under extension is very different from shear flow and at the same time less well understood. Extensional properties are traditionally hard to measure; however, one relatively simple method to simulate to behavior of a fluid in extensional flow is through applying an exponentially increasing shear.

Using a laboratory rheometer, the shear rate applied to a sample will be increased exponentially, creating strong flows comparable to those experienced in flow through porous media. Correlation between the rheological properties of the fluid under exponential flow to the formation damage potential of the fluid will be made.

Introduction

Improper polymer selection has been shown to cause significant formation damage in some situations[1,2]. Polymers can exhibit high rock retention and impede the flow of hydrocarbon from the formation due to blockages. Biopolymers are generally removed through acidization, breaking down the polymer backbone. Polymers can also be extruded into the pore spaces leading to a high increase in extensional viscosity. This increase in extensional viscosity can lead to an increase in formation damage by making it more difficult to remove the polymers from the pore spaces[3,4]. This damage can be minimized by the proper selection of polymers with good viscosification / suspension properties but with low extensional viscosities. This can be controlled by the architecture of the polymer chosen for the fluid, where branched polymers show greatly reduced formation damage and linear polymers show an increase in damage.

There were two types of fluids examined: brine/polymer mixtures and full formulation drill-in fluids. Brine / polymer solutions allowed the effect of polymer on the formation to be isolated, while using the full drill-in fluid formulation allowed an investigation into whether other components (i.e. bridging particles, fluid loss control polymers) had an effect on the formation damage and the extensional viscosity. An exponentially increasing shear flow was used as an approximation of extensional measurements, connecting the behavior of the flow in the porous formation to the potential for formation damage.

Extensional Flows and Exponential Shear

The rheological properties of fluids are often controlled by certain polymer characteristics including molecular weight, concentration, charge density and chain conformation[5,6]. The effect of these properties on the shear flow viscosity and the viscoelastic properties (storage and loss moduli) has been investigated for several decades. The effect of these properties on the extensional viscosity has been less well documented, especially in regard to water soluble polymers such as those used in wellbore construction. Exponential shear has been previously well-described in literature as a means of producing a "strong flow" in simulation of extension[7]. While several papers have demonstrated that chain extension in exponential shear is not as large as in planar extension for certain polymers melts (due to the mixed stretching and rotational of polymer chains in a rotational test)[8,9], little work has been done on dilute polymer solutions. In addition, the mix of elongation and shear experienced in the exponentially increasing flow mimics the same flows experienced in converging and diverging flows within porous media.

Exponential shear producing ideal strong flows would follow the form:

$$\gamma(t) = Ae^{\alpha t} - \frac{1}{A}e^{-\alpha t} \quad (1)$$

However, for simplicity, Equation 1 is reduced with minimal error to

$$\gamma(t) = A(e^{\alpha t} - 1) \quad (2)$$

and thus the shear rate also increases exponentially over time, as

$$\dot{\gamma}(t) = \alpha A e^{\alpha t} \quad (3)$$

In these equations, the parameter A is the "strain scale factor" and α is the "exponential rate constant". For a series of constant α, increasing A will result in increasing the maximum strain experienced. If A is held constant, increasing α will increase the acceleration of the shear rate through the test. Evaluation of the brine / polymer solutions at high strains and high acceleration for evidence of strain hardening or softening

of the polymers will reveal how the polymer chains stretch and fold in porous flows. This connection of polymer behavior in porous flows with both the chemistry of the brine / polymer fluid and the potential for formation damage will allow for both better prediction of damage and better design of fluids for contact with the reservoir.

Several choices for material functions have been proposed in literature: the two focused on here are listed below.

1) **Exponential Shear Stress Coefficient:** This is the instantaneous stress scaled by the instantaneous shear rate in an exponential shear flow. More simply, this can be thought of as the "exponential viscosity".

$$\eta^e(t) = \frac{\sigma^e(\alpha,t)}{\dot{\gamma}(t)} \tag{4}$$

2) **Principal Exponential Stress Growth Coefficient:** This function combines the shear and normal stresses. It can be thought of as the "principal exponential viscosity", or the viscosity along the first principal stress vector (which is not necessarily the direction of applied shear).

$$\eta_1^e(t) = \frac{\sqrt{N_1^e(t)^2+4\sigma^e(t)^2}}{2\dot{\gamma}(t)} \tag{5}$$

For a Newtonian fluid, these material functions are identical and rise monotonically, approaching a limiting value at long times. For viscoelastic fluids, the exponential viscosity has been thought to rise to a maximum and then decreases with time[10]. However, in practice, the effects of chain stretching and stain hardening at high values of α may cause the exponential viscosity to no longer decrease and plateau at long times. In addition, the behavior of the principal exponential viscosity, which for a simple viscoelastic fluid decreases monotonically over time, can exhibit non-monotonic behavior at long times when accelerated at higher values of α.

Flows in Porous Media

Because we are attempting to tie the rheological behavior of a fluid to its behavior when flowing in porous media, it is of interest to understand the conditions of shear in the pore. A standard assumption for diverging and converging flows such as experienced in porous media is that the shear rate in the pore is identical to the extensional rate experienced by the fluid. In order to estimate the shear rate, the Kozney-Carman model was used. In this model the flow is viewed as through a bundle of tortuous tubes of various sizes, with the tortuosity applied to both the effective length of the tubes and to the average velocity in the tube. Equation 6 gives the Kozney-Carman relation for velocity in the pore, based on fluid rheology and the assumed tortuosity and shape of the pores[11,12]. The shear stress at the wall can then be calculated from Equation 7 with the pressure drop, tortuosity, and the hydraulic radius of an average pore (based on permeability, porosity, shape, and tortuosity in Equation 8).

$$\frac{\langle u\rangle-\bar{u}_w}{r_H} = \frac{(1+\xi)\tau_{KC}}{k_0}\left(\frac{\sigma}{\tau_{KC}}\right)^{-\xi}\int_0^{\frac{\sigma}{\tau_{KC}}}\sigma^{(\xi-1)}f(\sigma)\,d\sigma \tag{6}$$

$$\bar{\sigma}_w = \frac{r_H}{\tau_{KC}}\left(\frac{\Delta P}{L}\right) \tag{7}$$

$$r_H = \sqrt{\frac{k k_0 \tau_{KC}^2}{\phi}} \tag{8}$$

With this set of equations fluid velocity in the pore can be calculated. The average shear rate in the pore can be calculated by

$$\dot{\gamma} = f(\sigma) = \frac{k_0(1+\xi n^*)}{(1+\xi)\tau_{KC} n^*}\left(\frac{\langle u\rangle-\bar{u}_w}{r_H}\right) \tag{9}$$

where n* is a correction for non-linearity in the stress function and is defined as

$$n^* = \frac{d\ln\bar{\sigma}_w}{d\ln\left[\frac{2(\langle u\rangle-\bar{u}_w)}{r_H}\right]} \tag{10}$$

Thus, if the permeability and porosity of the formation are known, along with basic fluid behavior defined by a rheological model, then the shear rate can be calculated as a function of pressure drop over a length of formation. These shear rates can then be compared to results from exponential shear tests to evaluate the effects on polymers in flow in porous media.

Fluids to be tested will generally fall under one of two rheological regimes – pseudoplastic or viscoplastic – requiring very different rheological models for use in conjunction with the Kozney-Carman model. Viscoplastic fluids will exhibit yielding behavior along with some degree of shear thinning. Pseudoplastic, or shear thinning, fluids will not exhibit a yield stress, but may have different features. For pseudoplastic fluids with an observable lower-Newtonian region, flow in pores will be modeled with a combination of the Kozney-Carman model with the Ellis model describing the rheology (chosen because it works well with the given system of equations). The Ellis model is a three-parameter model which well-describes the shear characteristics of these fluids, with the model given by:

$$\frac{1}{\eta} = \frac{1}{\eta_o}\left[1+\left(\frac{\sigma}{\sigma_2}\right)^{\alpha_E-1}\right] \tag{11}$$

where η_0 is the zero-shear viscosity in the lower-Newtonian region, α_E is a shear-thinning index, and σ_2 is roughly identified as the shear stress value at which η has fallen to half its final asymptotic value. By combining the Ellis model with the Kozney-Carman model for flow in porous media, Equation 6 becomes:

$$\frac{\langle u\rangle-\bar{u}_w}{r_H} = \frac{\bar{\sigma}_w}{k_0\eta_o}\left[1+\left(\frac{(1+\xi)}{(\alpha_E+\xi)}\right)\left(\frac{\bar{\sigma}_w}{\tau_{KC}\sigma_2}\right)^{\alpha_E-1}\right] \tag{12}$$

Thus, the shear rate can be determined as

$$\dot{\gamma} = \frac{(1+\xi n^*)\bar{\sigma}_w}{(1+\xi)\tau_{KC} n^*\eta_o}\left[1+\left(\frac{(1+\xi)}{(\alpha_E+\xi)}\right)\left(\frac{\bar{\sigma}_w}{\tau_{KC}\sigma_2}\right)^{\alpha_E-1}\right] \tag{13}$$

In the case of a viscoplastic fluid which exhibits a yield stress, two models are available for use – the Bingham plastic and Casson models. More focus is given to the Cason model, which is similar to the Bingham plastic model except that the parameters, the stress, and the shear rate are raised to the

power of ½. This gives the model more flexibility to better fit empirical data for fluids exhibiting both shear-thinning and yielding characteristics.

$$\sigma^{1/2} = \sigma_0^{1/2} + \eta_1^{1/2}\dot{\gamma}^{1/2} \quad (14)$$

In this case, Equations 6 and 9 becomes:

$$\frac{\langle u\rangle - \bar{u}_w}{r_H} = \frac{\tau_{KC}(1+\xi)}{k_0\eta_1}\left(\frac{\sigma_0}{\xi} - \frac{2\sigma_0^{1/2}}{(1/2+\xi)}\left(\frac{\bar{\sigma}_w}{\tau_{KC}}\right)^{1/2} + \frac{\bar{\sigma}_w}{\tau_{KC}(1+\xi)}\right) \quad (15)$$

$$\dot{\gamma} = \frac{(1+\xi n^*)}{n^*\eta_1}\left(\frac{\sigma_0}{\xi} - \frac{2\sigma_0^{1/2}}{(1/2+\xi)}\left(\frac{\bar{\sigma}_w}{\tau_{KC}}\right)^{1/2} + \frac{\bar{\sigma}_w}{\tau_{KC}(1+\xi)}\right) \quad (16)$$

At relatively high shear rates in this model, n* approaches 1; however, at stresses near the yield stress the model actually predicts decreasing shear rate with increasing shear stress. The stress inflection point for Equation 16 is found to be dependent only on the yield stress, σ_0, and the assumed geometry of the pores (τ_{KC}, k_0, and ξ). For the Kozney-Carman parameters, the stress inflection point is at $1.85\sigma_0$.

In addition to the interest in the shear rate (and thus extensional rate) in the pores, it is also of interest to determine Reynolds number for flow in the pore, to evaluate the flow regime in the pore. The Reynolds number for a porous bed is given by [Kazicki and Tiu 1988]

$$Re_P^* = \frac{D_P\phi(\langle u\rangle - \bar{u}_w)\rho}{\eta_D(1-\phi)} \quad (17)$$

where D_P is the bed particle diameter, ρ is the fluid density, and η_D is the Darcy viscosity for non-Newtonian flows in porous media, given by

$$\frac{\langle u\rangle - \bar{u}_w}{r_H} = \frac{\bar{\sigma}_w}{k_0\eta_D} \quad (18)$$

The bed particle diameter is related to the hydraulic radius and the bed column diameter, D_C, by the following

$$r_H = \frac{\phi D_P}{6(1-\phi)+4\left(D_P/D_C\right)} \quad (19)$$

However, since D_C can be considered much greater than D_P or r_H that term can be neglected. For operation in the laminar regime, Re_P^* should be less than 5-10, while fully turbulent flow is observed when Re_P^* is above 2000.

Experimental Methods

Testing performed for the data presented in this paper were done in the same method as described in SPE 151889 by Maxey and van Zanten[13]. The formation damage caused by the fluids was tested using an in-house Automated Return Permeameter (ARP) using ~100 mD Berea sandstone cores. The testing procedure was as follows:

Core

1. Drill 1 ½" diameter, >2" length core from sandstone block
2. Dry for >16 hours in an over at 215°F
3. Obtain weight, diameter and length for dry core
4. Saturate in 5 wt-% NaCl under vacuum for 2 hours
5. Soak for >16 hours in 5 wt-% NaCl
6. Obtain weight of saturated core
7. Calculate pore volume from dry/saturated weight

Oil premeability testing – polymer/brine solution

1. Load the brine saturated core into Automated Return Permeameter
2. Raise confining pressure to 1000psi and temperature to 200°F
3. Flow Soltrol at 4mL/min until permeability is stable
4. Record initial permeability
5. Displace the damaging fluid to the face of the core
6. Run damage with 50psi of differential pressure for 2 pore volumes using dynamic filtration.
7. Flow Soltrol at 4mL/min until permeability is stable
8. Record the permeability difference as regain permeability

Oil premeability testing – drill-in fluid

1. Load the brine saturated core into Automated Return Permeameter
2. Raise confining pressure to 1000psi and temperature to 200°F
3. Flow Soltrol at 4mL/min until permeability is stable
4. Record initial permeability
5. Displace the damaging fluid to the face of the core
6. Run damage with 500psi of differential pressure for 2 hours using dynamic filtration.
7. Flow Soltrol at 4mL/min until permeability is stable
8. Record the permeability difference as regain permeability

Exponential shear and other rheological tests were performed on an Anton Paar MCR501 rheometer using a cone-and-plate geometry (50-mm diameter, 1° cone angle) or sandblasted 50-mm parallel plates at a gap of 0.5-mm. All rheological tests were conducted at 120°F

Results and Discussion

Initially the regain permeability of a brine/polymer system was investigated to differentiate between the damaging effects of various polymers. Initially, two common biopolymer systems were looked at, one that was linear (in 14.0ppg $CaCl_2/CaBr_2$ brine – Linear Biopolymer #1) and one that contained extensive branching (in 9.5ppg KCl/NaCl brine – Branched Biopolymer). The regain permeability results are shown in Figure 1.

The regain permebility for Linear Polymer #1 was seen to be 25% while the Branched Polymer was seen to be 35%. A hyperbranched synthetic polymer was also investigated (in 14.0ppg $CaCl_2/CaBr_2$ brine – Hyperbranched Polymer) and the regain permeability was seen to be 55%. By examining the damage effects of the Hyperbranched Polymer and Linear Biopolymer #1 in the same brine, it is possible to eliminate artifacts induced by brine type. It is readily apparent that flooding the formation with any high molecular weight polymer can cause extensive damage, thus in field applications a breaker is usually included or a remedial treatment is performed. All systems showed extensive damage, however

the Linear Biopolymer #1 with its higher extensional viscosity showed higher relative damage. Several regain permeability tests were performed using various brine based fluids with the Branched Biopolymer consistently showing an approximately 10% higher regain permeability. This evidence supports the damage mechanism by extrusion of the polymer into the formation creating a higher extensional viscosity.

Drill-in fluids were also looked at in order to determine if these effects are still relevant with the addition of the varied components in these fluids. A general formulation was followed and is shown in Table 1.

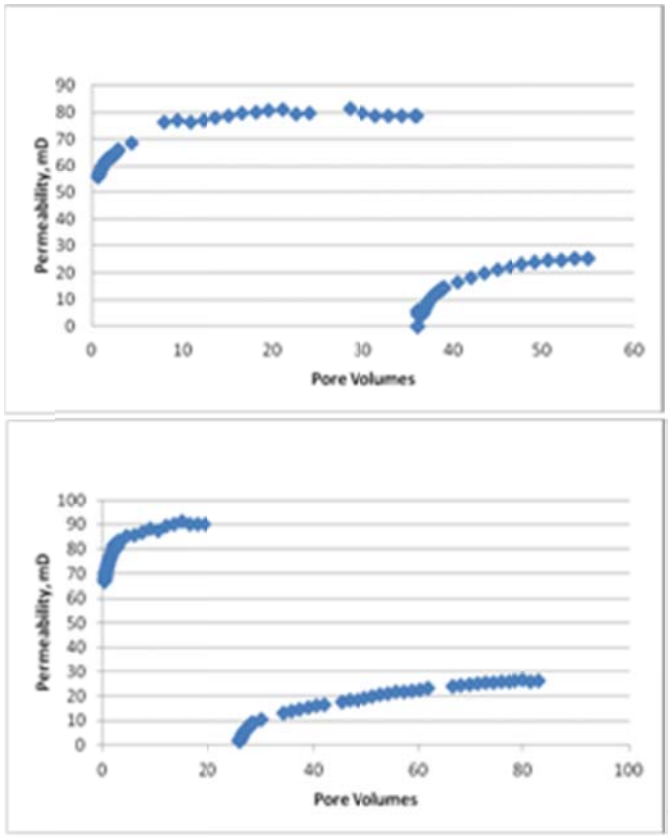

Figure 1 Regain permeability results of Branched Biopolymer (a) and Linear Biopolymer #1 (b) when tested as just polymer in brine.

Table 1 Standard drill-in fluid formulation.

Brine (bbl)	0.950
Defoamer (ppb)	0.175
Viscosifier (ppb)	1.25
Fluid loss starch (ppb)	6
Alkalinity agent (ppb)	1
Calcium carbonate (ppb)	40

The regain permeability results for the Linear Biopolymer #1 Drill-In fluid are shown below in Figure 2. It is readily apparent that the regain permeability is greatly enhanced by the addition of the other components in the drill-in fluid. The Linear Biopolymer #1 drill-in fluid had a regain permeability of 75% and the Branched Biopolymer fluid had a regain permeability of 85%. This is consitent with the polymer/brine results, with the absolute regain permeability being much higher for the drill-in fluids. Drill-in fluids are designed to be non-invasive, and thus causing low damage, through the introduction of specific materials. These materials such as calcium carbonate bridging material to bridge off the pore throats and fluid loss control polymer to minimize fluid invasion greatly reduce the damage mechanisms such as particle plugging. They also limited the depth in which the viscosifying polymer can penetrate the formation, thus reducing the damage. Thus the Linear Biopolymer #1 was consistently more damaging than the Branched Biopolymer and Hyperbranched Polymer as summarized in Figure 3.

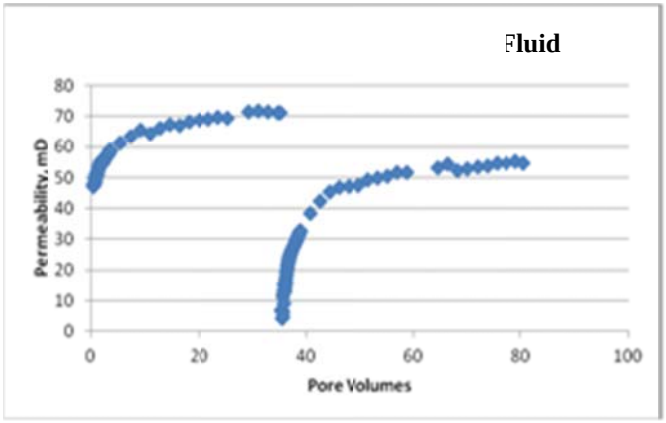

Figure 2 Regain permeability of a Linear Biopolymer #1 when formulated in a complete drill-in fluid.

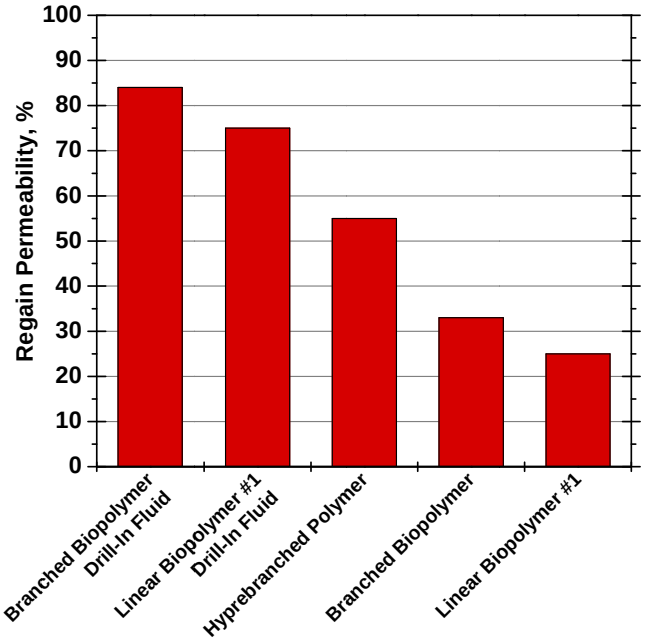

Figure 3 Regain permeability comparison of the linear versus branched biopolymer fluids.

The flow curves of the three fluids when tested at 120°F are presented in Figure 4a. In addition to the three prior fluids, two additional fluids are compared – Linear Biopolymer #1 in 9.5ppg KCl/NaCl brine and a second linear biopolymer, Linear Biopolymer #2 in 14.0ppg $CaCl_2/CaBr_2$ brine. The flow curves reveal that two of the tested fluids, the

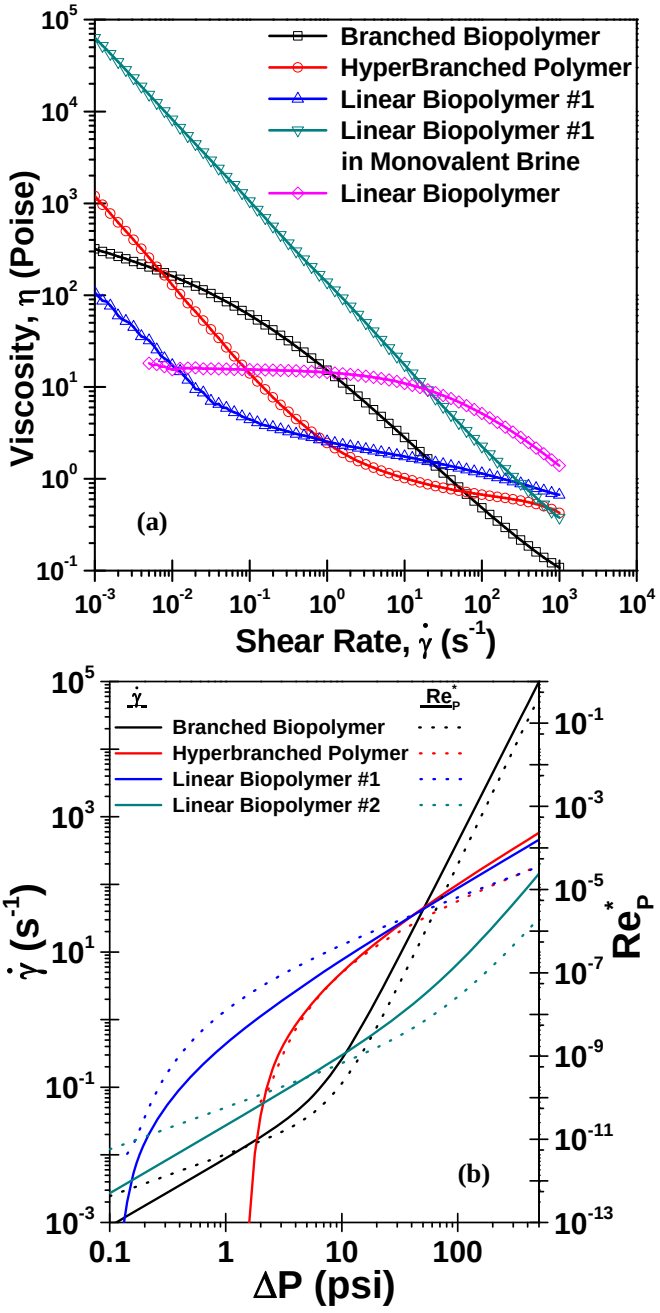

Figure 4 (a) Flow curves of the test fluids at 120°F. (b) Predicted shear rate, $\dot{\gamma}$, and Reynolds number, $\mathbf{Re}_P^*$, in the pore using the Kozney-Carman model for three test fluids.

Hyperbranched Polymer and Linear Biopolymer #1, exhibit very weak yielding characteristics while the remaining three are pseudoplastic and, for the Branched Biopolymer and Linear Biopolymer #2, show signs of a lower Newtonian viscosity at very low shear rates. In addition, the Hyperbranched Polymer and Linear Biopolymer #1 have a relatively similar viscosity and shear-thinning profile at higher shear rates, while the Branched Biopolymer is significantly more shear-thinning and has a much lower viscosity at very high shear rates. For predicting shear rates of the fluids in the pore as a function of pressure drop, the Ellis model was used for the pseudoplastic systems, while those with yielding, viscoplastic behavior were modeled using the Casson model.

The predicted shear rate and Reynolds number in the pore using the Kozney-Carman model for three fluids tested is presented in Figure 4b. Each was evaluated at the initial core permeability observed in the regain permeability tests ILinear Biopolymer #2 at 75-mD), assuming a porosity of 15% and a pressure drop across a 2-inch length (the length of the core samples used in testing). As expected from the observing the viscosity of the fluids in the flow curves, the Branched Biopolymer is expected to experience both higher shear rates and flow at higher Reynolds numbers at pressure drops above 50-psi in the core test. At the test differential pressure of 500-psi (used for the drill-in fluid formulations), the Hyperbranched Biopolymer and Linear biopolymer #1 would be expected to have an average shear rate of ~500 s^{-1} in the pore, while the Linear Biopolymer #2 would have a shear rate of ~100 s^{-1} and Branched Biopolymer fluid would have a shear rate as high as ~10,000 s^{-1}. However, even at this extremely high predicted shear rate, Re_P^* remains below ~0.5, well within the fully laminar flow region. For the permeability tests with polymer / brine fluids, where a lower pressure differential of 50-psi was used, the shear rate for all three fluids tested in the permeameter are equal, at 42 s^{-1}, and Re_P^* is ~10^{-6}. (For the Linear Biopolymer #2, these would be ~2 s^{-1} and Re_P^* ~10^{-8} for a 50-psi differential.) This would indicate that even with the potential for high shear rates in the formation pores at high differential pressures, there is little likelihood of turbulent flows causing mechanical breakages of the rock which would lead to blockages. Therefore, any resultant formation damage in these tests can be viewed as a direct result of polymer behavior.

From the regain permeability results, it is easy to draw a conclusion that degree of chain branching has some effect on the total damage done to a formation by the polymer. Exponential shear tests were performed to further evaluate a rheological motivation for the induced damage, which could then be applied to polymer solution or to other non-polymeric fluids. The results of exponential shear tests on the polymer / brine fluids at constant values of A=1 and increasing α from 0.01 to 1 are presented in Figures 5 and 6. Several similarities and differences can be observed between the fluids. First, for the Branched Biopolymer (Figure 5a) the instantaneous exponential viscosity, η^e, is observed to initially increase with strain (e.g. the effective pore length over which shear has been experienced) regardless of the value of α, the acceleration rate of the shear, used for the test. At a common strain of ~1, the

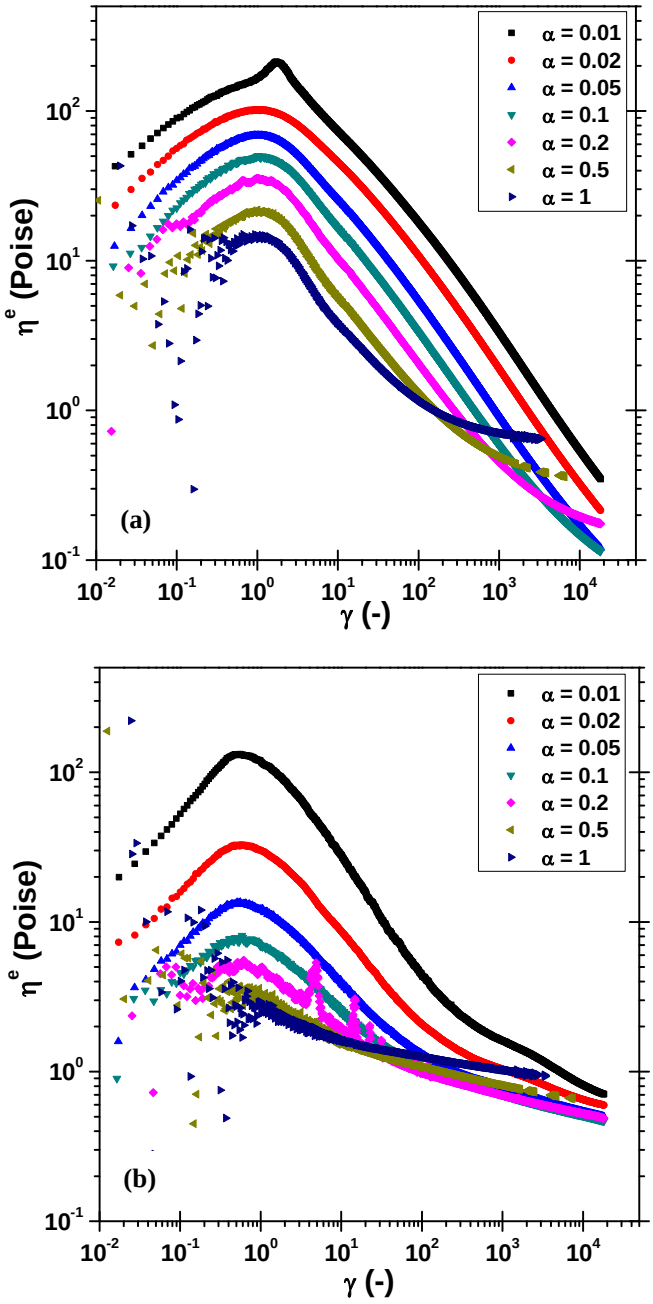

Figure 5 The instantaneous exponential viscosity, η^e, as a function of increasing strain for (a) the Branched Biopolymer in monovalent brine and (b) the Hyperbranched Polymer in divalent brine. For each fluid tests were conducted at a temperature of 120°F and the strain scale factor, A, was held constant at 1 while the exponential rate constant, α, was increased from 0.01 to 1.

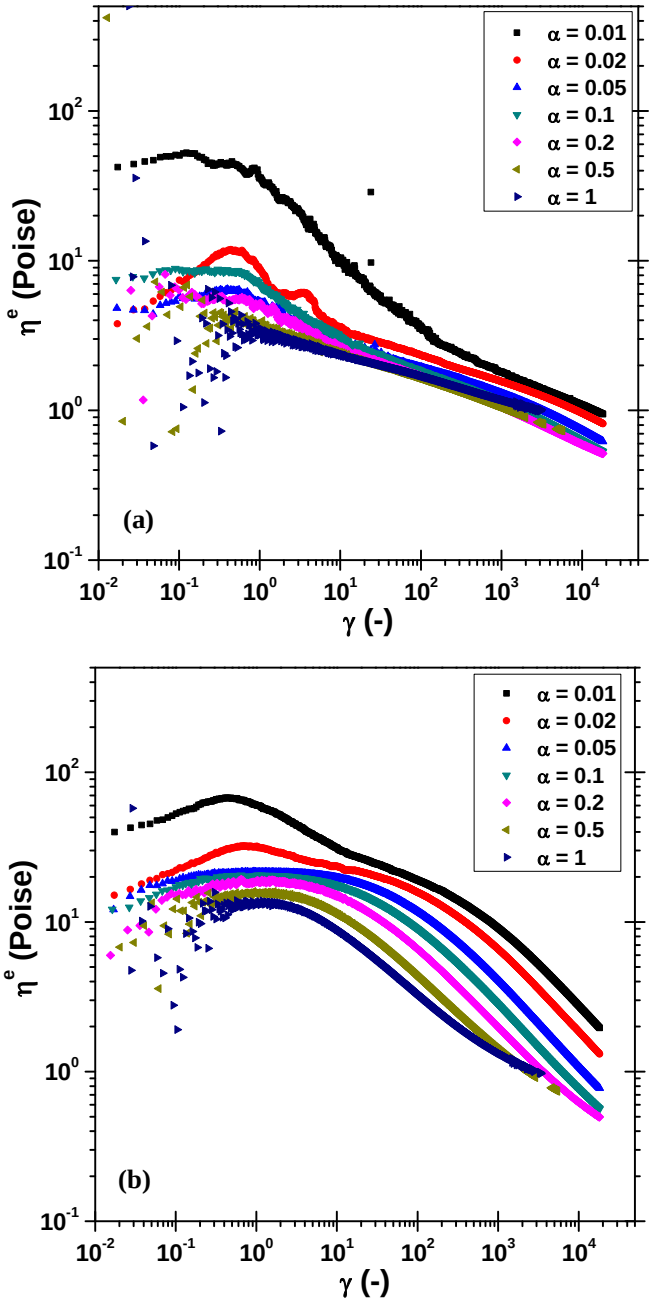

Figure 6 The instantaneous exponential viscosity, η^e, as a function of increasing strain for (a) Linear Biopolymer #1 in divalent brine and (b) Linear Biopolymer #2 in divalent brine. For each fluid tests were conducted at a temperature of 120°F and the strain scale factor, A, was held constant at 1 while the exponential rate constant, α, was increased from 0.01 to 1.

exponential viscosity reaches a peak and begins to decrease with strain; since strain rate is also increasing with the increasing strain, this is observed as a simple shear-thinning response. However, at higher acceleration rates this shear-thinning behavior slows and η^e beings to plateau at high values of strain. This is a strain-hardening effect, where at very high strains the stretching of the polymer chains begins to hinder further flow. From this is can be surmised that the extensional viscosity in the pore is increasing, also due to chain stretching, thus preventing the invasion of the polymer chain into the

pore.

For the Hyperbranched Polymer, the same increase in η^e through a strain of ~1 is observed; however, at higher acceleration rates the peak becomes muted and eventually vanishes. Also, for moderate acceleration rates η^e tends to collapse onto a single line at high strains; since the shear rate for a particular strain is higher when the acceleration rate is higher, this coalescence of viscosity/strain curves translates to increasing viscosity for a common shear rate. Again, as in the Branched Biopolymer, strain-hardening is observed at the highest acceleration rates.

When considering Linear Biopolymer #1 (Figure 6a), we do not observe the same peak in exponential viscosity at low strains as seen in the Branched and Hyperbranched Polymer fluids. This is not simply a function of the shear viscosity of Linear Biopolymer #1 fluid, as it is very similar to that of the Hyperbranched Polymer fluid, and must be a function of the polymer chain and/or its interaction with the brine. In addition, at high strains shear-thinning continues – even at the highest accelerations rates. No strain-hardening is observed in the Linear Biopolymer #1 / brine fluid system. This lack of strain-hardening (e.g. lack of increased resistance of the polymer chains to flow over long distances through the pore) translates into an ability for Linear Biopolymer #1 to penetrate further into the formation, thus increasing interactions of the polymer with the formation (absorption onto the pore walls) and increasing the difficulty of removing the linear polymer from the formation and decreasing the observed regain permeability.

By comparison, Linear Biopolymer #2 exhibits several similarities in exponential shear tests to Linear Biopolymer #1. While the data at different acceleration rates do not quite collapse onto a single curve as in Linear Biopolymer #1, there is the same consistent shear-thinning at high strains. At the highest acceleration rates, at very high strains, there is a small positive inflection indicating some strain hardening, but not nearly to the degree observed in the Branched and Hyperbranched Polymer fluids. While not yet tested in the permeameter, this fluid would be expected to perform marginally better than Linear Biopolymer #1, but not as well at the Branched or Hyperbranched Polymer fluids.

By way of comparison of the effects of brine on the polymer fluid, exponential shear tests were also conducted on Linear Biopolymer #1 in monovalent brine, 9.5ppg KCl/NaCl, using the same polymer loading as in the divalent brine tests. The flow curve for this fluid can be seen in Figure 4a, and the exponential viscosity as a function of strain for this system is presented in Figure 7. By changing the brine, and thus the charge screening effects on the Linear Biopolymer #1 chain, the rheological properties of the fluid were dramatically changed. Unlike when tested in divalent brine, Linear Biopolymer #1 in monovalent brine exhibits very similar exponential shear results as does the Branched Biopolymer in monovalent brine. A defined exponential viscosity peak is observed at strain of ~1, as well as the onset of a plateau in η^e at high strain and high acceleration rates. However, the degree of strain-hardening observed is not as great as in the Branched or Hyperbranched Polymer fluids; this likely indicates that Linear Biopolymer #1 in monovalent brine would exhibit improved regain permeability results, but still not as high as observed in the Branched or Hyperbranched Polymer fluids.

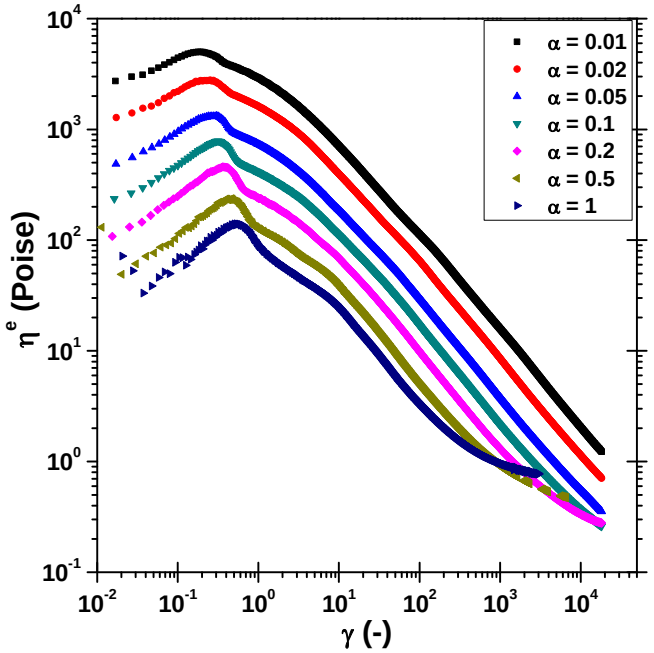

Figure 7 The instantaneous exponential viscosity, η^e, as a function of increasing strain for the linear biopolymer in monovalent brine at 120°F.

A comparison of the instantaneous exponential viscosity for the four polymer / brine fluids, plus for Linear Biopolymer #1 in monovalent brine, at a common acceleration rate of $\alpha = 0.5$ is presented in Figure 8. From this a basis for modeling the formation damage from exponential shear tests can be begun. These curves were produced at two different values of the strain scale factor, with A = 0.1 and A = 10, the results of which overlapped well to produce a single continuous curve. The previously noted appearance of strain hardening in the Branched and Hyperbranched Polymer fluids is again evident, with the Hyperbranched Polymer fluid showing a positive inflecting indicating strain hardening at lower strain (γ = ~6) than any other fluid. The Branched Biopolymer fluid shows inflection at a strain of γ = ~200. Both of these also exhibit increased stiffness at very high strains. Linear Biopolymer #1 never exhibits a positive inflection indicating strain hardening; instead, at the highest strains a negative inflection is observed indicating some degree of strain softening.

This progression follows that of the observed damage done to core samples in permeability testing:

Strain, γ, at which Strain Hardening Begins

Hyperbranched Polymer < Branched Biopolymer < Linear Biopolymer #1

Degree of Formation Damage Incurred

Hyperbranched Polymer < Branched Biopolymer < Linear Biopolymer #1

By following this trend we could predict that Linear Biopolymer #1 in monovalent brine, which shows a modest positive inflecting at γ = ~1000, would have produce less formation damage than when run in divalent brine but still not have a high a regain permeability as the Branched Biopolymer. Similarly, the tests on Linear Biopolymer #2 indicate a modest positive inflection at γ = ~3000, placing its potential for formation damage again between the Branched Biopolymer and Linear Biopolymer #1 in divalent brine and potentially marginally worse than Linear Biopolymer #1 in monovalent brine.

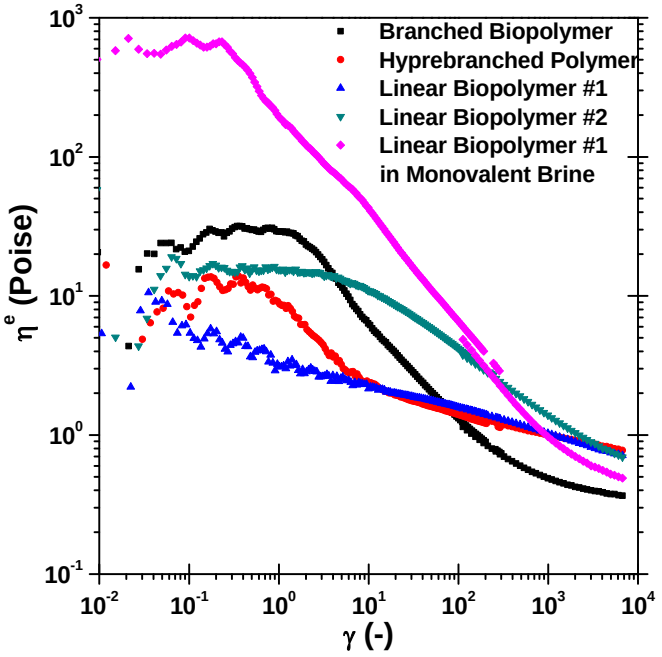

Figure 8 Comparison of the instantaneous exponential viscosity, η^e, for the various test fluids at a constant exponential rate of $\alpha = 0.5$.

Conclusions

- The degree of polymer branching affects the potential for a fluid to reduce the permeability of a formation.
- Rheological behavior of polymer solution in shear and extensional flows affects the flow of a fluid in porous media, and thus the potential for a fluid to reduce the permeability of a formation. As an analog for the mixed shear and extensional flows observed in porous media, exponentially increasing shear is potentially a good and fast measure for the degree of formation damage expected from a fluid.
- The onset of strain-hardening at moderate to high exponential acceleration rates in the Branched and Hyperbranched Polymer fluids are indicators of their lack of ability to deeply penetrate into the formation. In contrast, the lack of such strain-hardening in the Linear Biopolymer #1 in divalent brine indicates potential of greater penetration and thus greater damage to the formation.
- The selection of brine has an effect on the behavior of the polymer in flow through porous media. While the brine itself does not directly affect the degree of damage caused to a formation, it can affect the appearance of strain-hardening in different polymer systems and thus influence regain permeability.

Nomenclature

A = strain scale factor
D_C = porous bed column diameter
D_P = porous bed particle diameter
$f(\sigma)$ = function describing the relationship between shear rate and shear stress in a fluid
k = permeability
k_0 = shape factor in Kozeny-Carman model (=2.5)
L = length over which pressure drop is evaluated
ΔP = pressure drop
r_H = hydraulic radius of the pore
$\langle u \rangle$ = average velocity in the pore
$\bar{u}_w$ = velocity at the wall
α = exponential rate constant
α_E = shear-thinning index in the Ellis model
γ = strain
$\dot{\gamma}$ = strain rate
η = viscosity
η_0 = zero-shear viscosity in the Ellis model
η_1 = plastic viscosity in the Casson model
η_D = Darcy viscosity
ξ = aspect factor in Kozeny-Carman model (=3.0)
ρ = density
σ = shear stress, with an overbar and subscript w it indicates average stress at the wall
σ_0 = yield stress in the Casson model
σ_2 = the shear stress value at which η has fallen to half its final asymptotic value in the Ellis model
τ_{KC} = tortuosity in Kozeny-Carman model (=$\sqrt{2}$)
ϕ = porosity

Acknowledgments

The authors would like to thank Halliburton for permission to pursue and publish this research. We would also like to thank Gareth McKinley at MIT for helpful conversations in beginning to explore exponential shear.

References

1. Audibert, A., et al. 1999. "Role of Polymers in Formation Damage." SPE 54767 presented at the SPE European Formation Damage Conference, The Hague, The Netherlands, 31 May-1 June 2.
2. Javora, P.H., et al. 2000. "Viscosification of Oilfield Brines: Guidelines for the Prevention of Unexpected Formation Damage." SPE 58728 presented at the SPE International Symposium on Formation Damage Control, Lafayette, LA, USA, 23-24 February.
3. Jones, D.M. and K. Walters. 1988. "Extensional Viscosity Effects in EOR." SPE 18070 presented at the SPE Annual

Technical Conference and Exhibition, Houston, Texas, 2-5 October.
4. Svendsen, Ø., et al. 1998. "Optimum Fluid Design for Drilling and Cementing a Well Drilled with Coil Tubing Technology." SPE 50405 presented at the SPE International Conference on Horizontal Well Technology, Calgary, Alberta, Canada, 1-4 November.
5. Flory, P. 1953. *Principles of Polymer Chemistry*. Ithaca, NY: Cornell University Press.
6. Flory, P. 1969. *Statistical Mechanics of Chain Molecules*. New York, NY: Interscience.
7. Doshi, S.R. and J.M. Dealy. 1987. "Exponential Shear: A Strong Flow." *Journal of Rheology* **31**(7), 563-582.
8. Venerus, David C. 2000. "Exponential Shear Flow of Branched Polymer Melts." *Rheologica Acta* **39**, 71-79.
9. Kwan, T., et al. 2001. "An Experimental and Simulation Study of Dilute Polymer Solutions in Exponential Shear Flow: Comparison to Uniaxial and Planar Extensional Flows." *Journal of Rheology* **45**(2), 321-349.
10. Dealy, J.M. and R.G. Larson. 2006. *Structure and Rheology of Molten Polymers*. Hanser Publishers.
11. Kozicki, W. and C. Tiu. 1988. Parametric Modeling of Flow Geometries in Non-Newtonian Flows. *Encyclopedia of Fluid Mechanics: Rheology and Non-Newtonian Flows*. N.P. Cheremisinoff (ed.), Houston, TX: Gulf Publishing Co, **7**, 199-252.
12. Masuda, Y., et al. 1992. "1d Simulation of Polymer Flooding Including the Viscoelastic Effect of Polymer Solution." SPE 19499, *SPE Reservoir Engineering*, 247-252.
13. Maxey, J. and R. van Zanten. "Novel Method to Characterize Formation Damage Caused by Polymers." SPE 151889 presented at the SPE International Symposium and Exhibition on Formation Damage Control held in Lafayette, Louisiana, USA, 15–17 February 2012.